Electronic Supplementary Material (ESI) for Journal of Materials Chemistry A.

Electronic Supplementary Information for

Naturally tridimensional laminated porous carbon networks structured short nano-chains bridging nanospheres for energy storage

Chao Wang,[a] *Ye Xiong,*[a] *Hanwei Wang,*[a] *Chunde Jin,*[a] *Qingfeng Sun,*[a]*

[a] School of Engineering, Zhejiang A&F University, Hangzhou 311300, China.

* Correspongding author

* E-mail: qfsun@zafu.edu.cn

This file includes:

Figure S1 to Figure S13

Supplementary Note 1 to Note 3

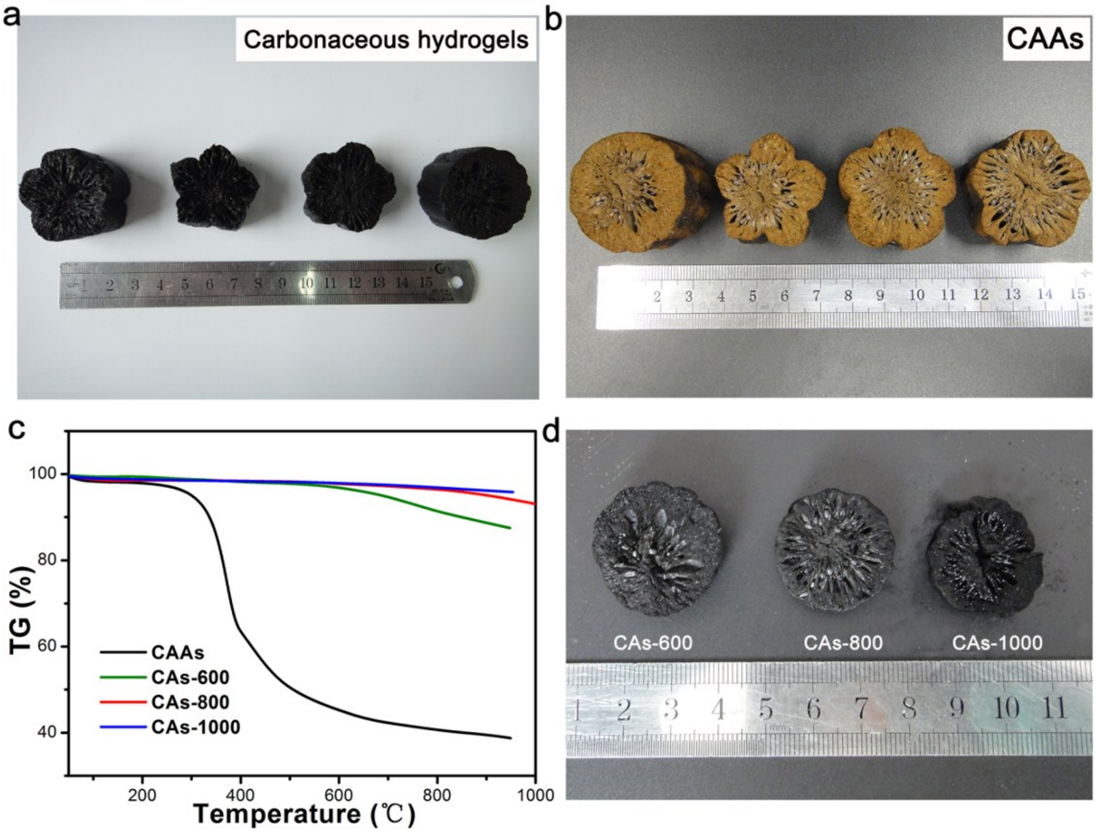

Figure S1. Photographs of carbonaceous hydrogels (a) and CAAs (b). (c) TGA curves of CAAs and CAs. (d) Photograph of CAs-600, CAs-800 and CAs-1000. (The size of CAs slightly decreases with the carbonized temperature increasing.)

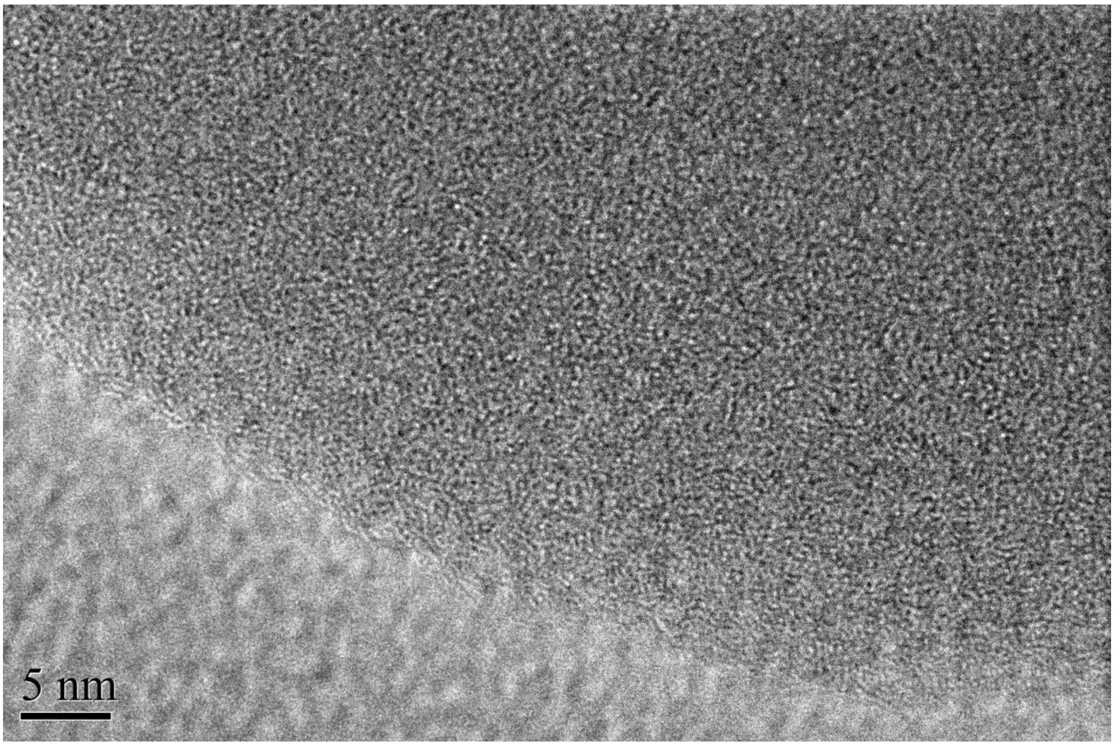

Figure S2. HR-TEM image of CAAs.

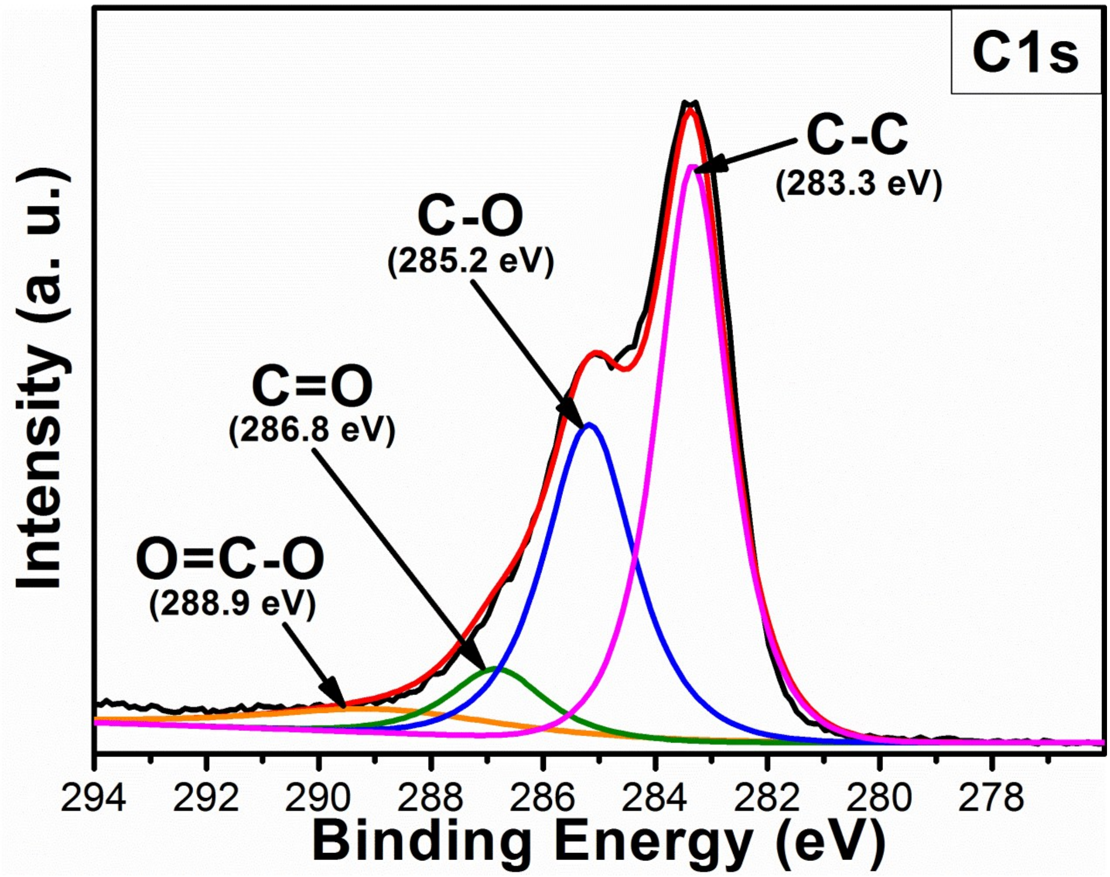

Figure S3. XPS C 1s high-resolution spectrum of CAAs.

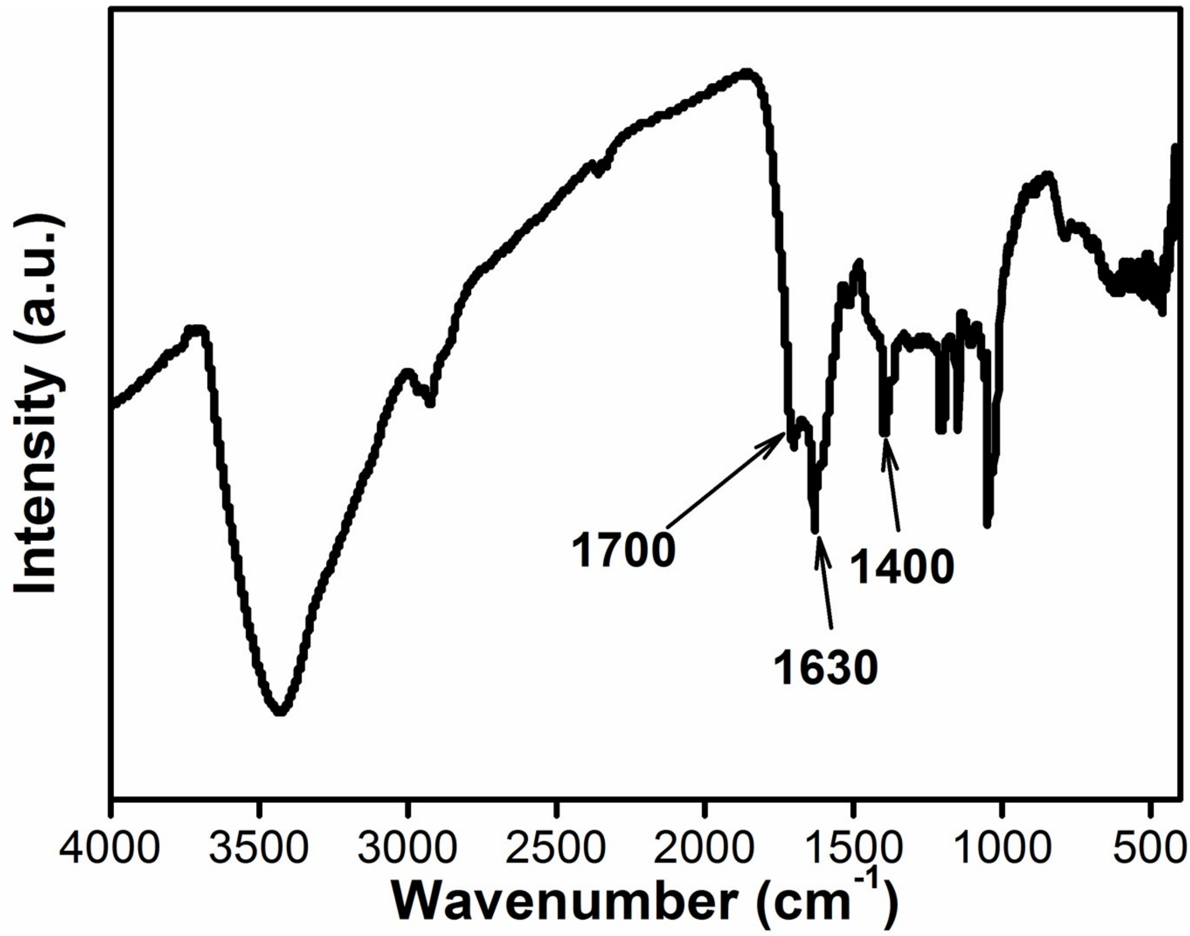

Figure S4. FTIR spectra of CAAs.

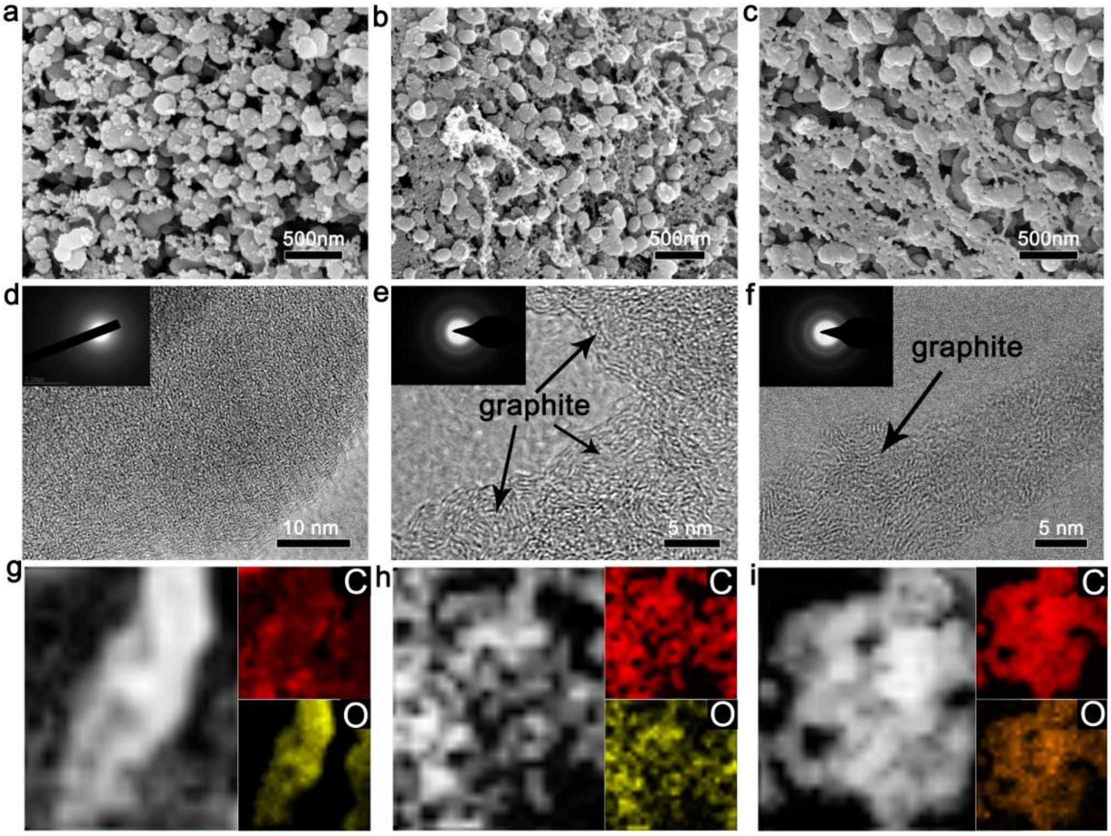

Figure S5. SEM images, HR-TEM images with diffraction patterns, and elemental mappings of CAs-600 (a, d and g), CAs-800 (b, e and h), and CAs-1000 (c, f and i), respectively.

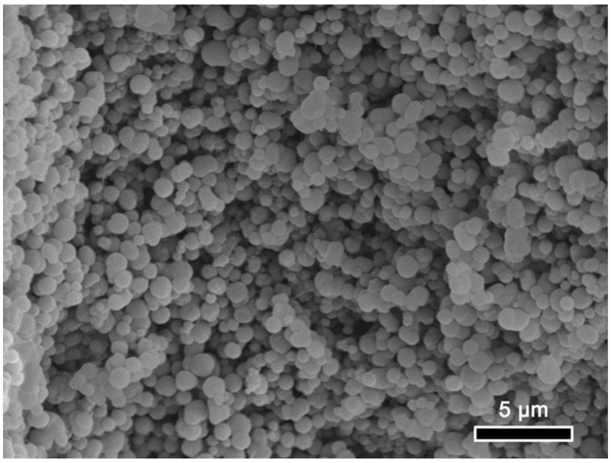

Figure S6. The SEM image of RFCS-600.

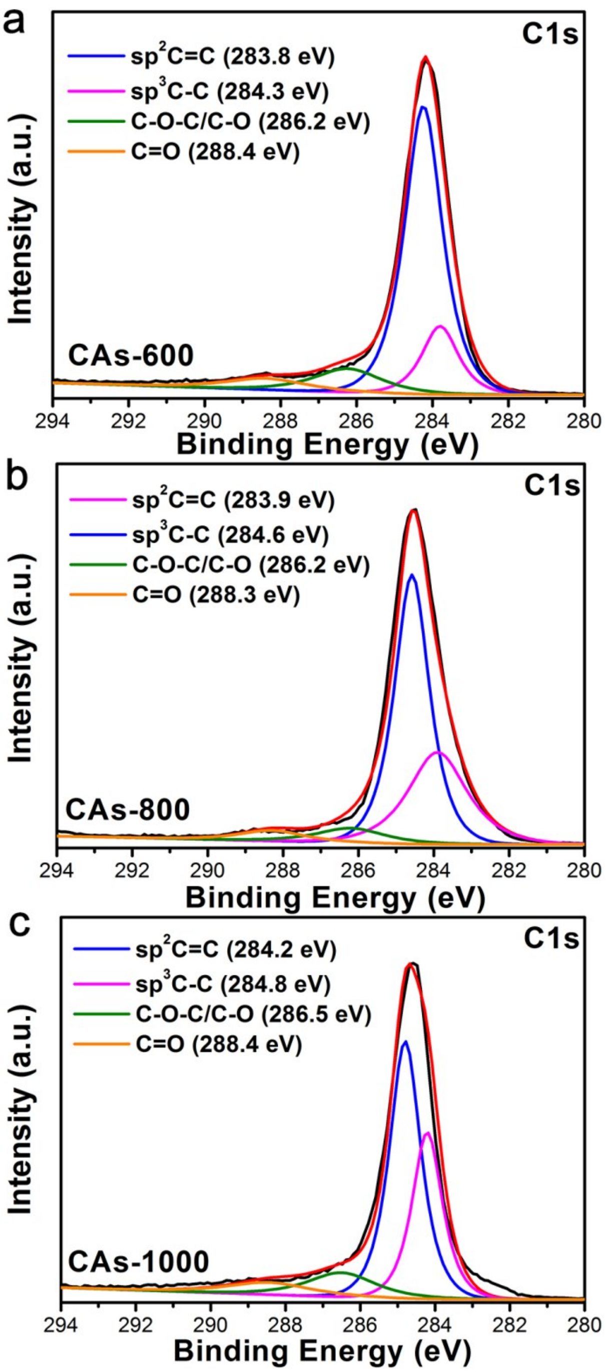

Figure S7. The XPS C 1s spectrums of CAs-600, CAs-800 and CAs-1000.

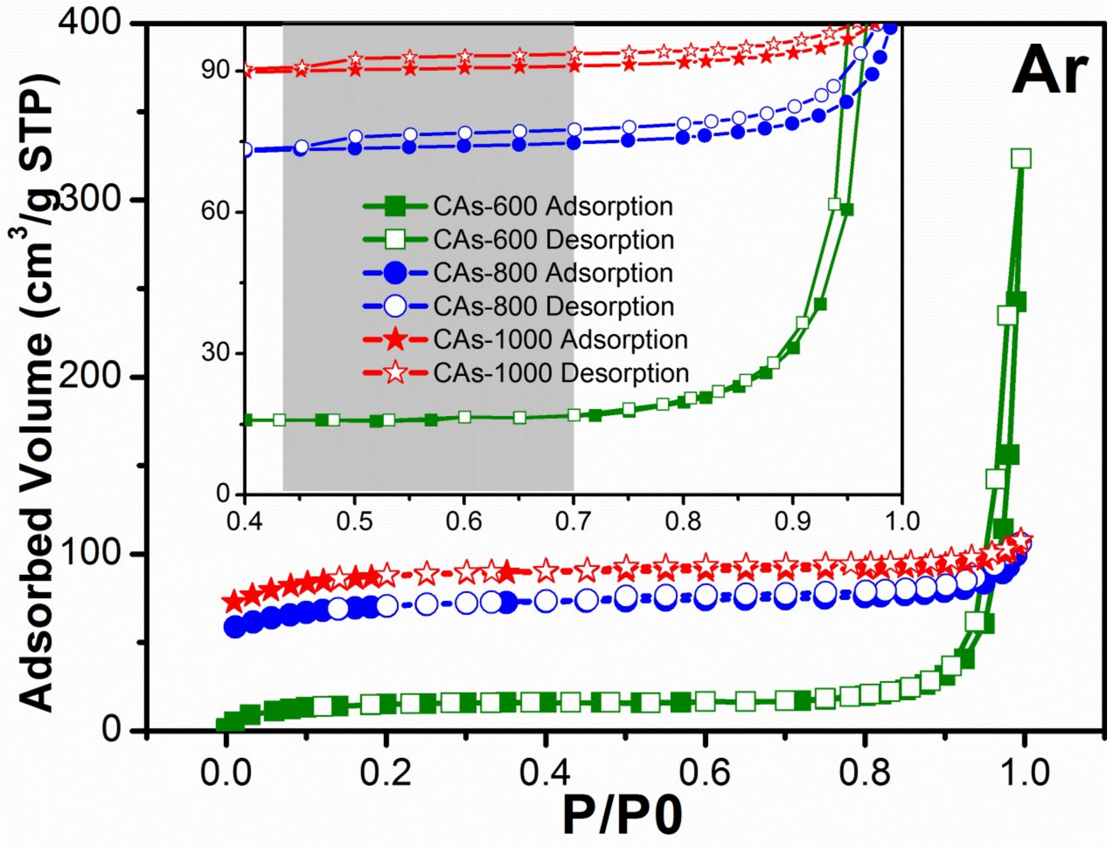

Figure S8. Ar adsorption desorption isotherms of CAs-600, CAs-800 and CAs-1000.

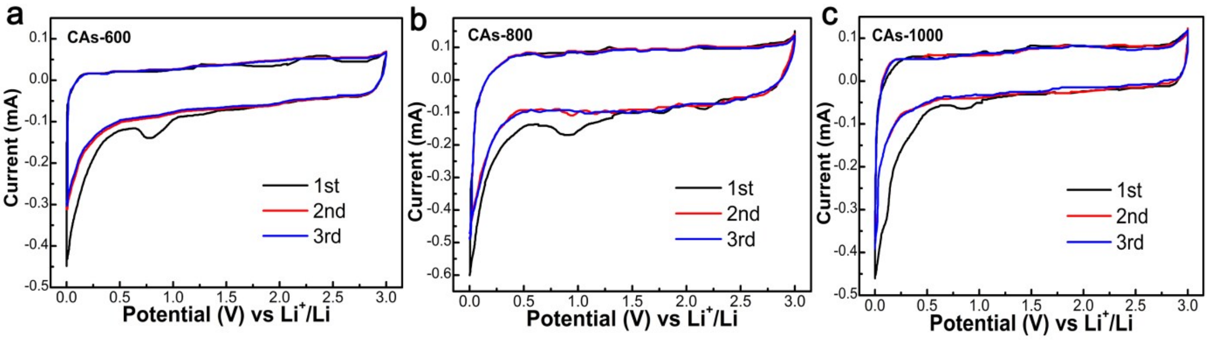

Figure S9. The Cyclic voltammetry curves of RFCS-600, CAs-600, CAs-800, and CAs-1000 for application of LIBs at the 100 mV s^{-1}.

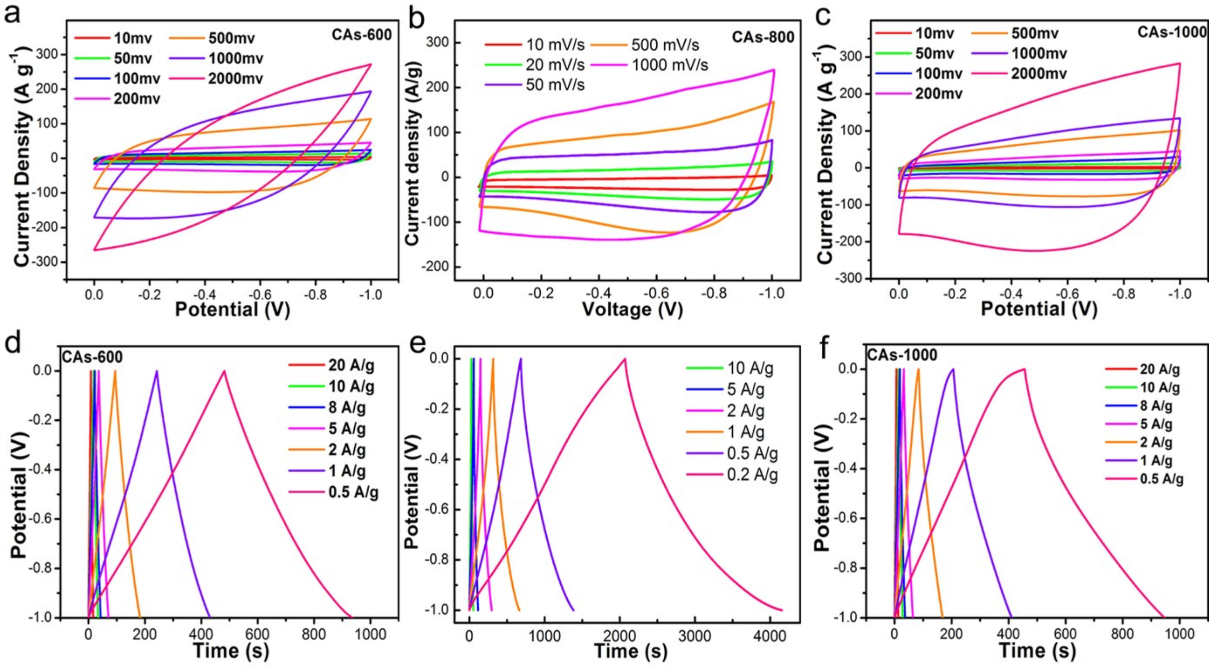

Figure S10. Cyclic voltammetry curves of CAs-600 (a), CAs-800 (b) and CAs-1000 (c) ranging from 10 to 2000 mv. Galvanostatic charge/discharge test data of CAs-600 (d), CAs-800 (e) and CAs-1000 (f) at scan rate from 0.5 to 20 A g^{-1}.

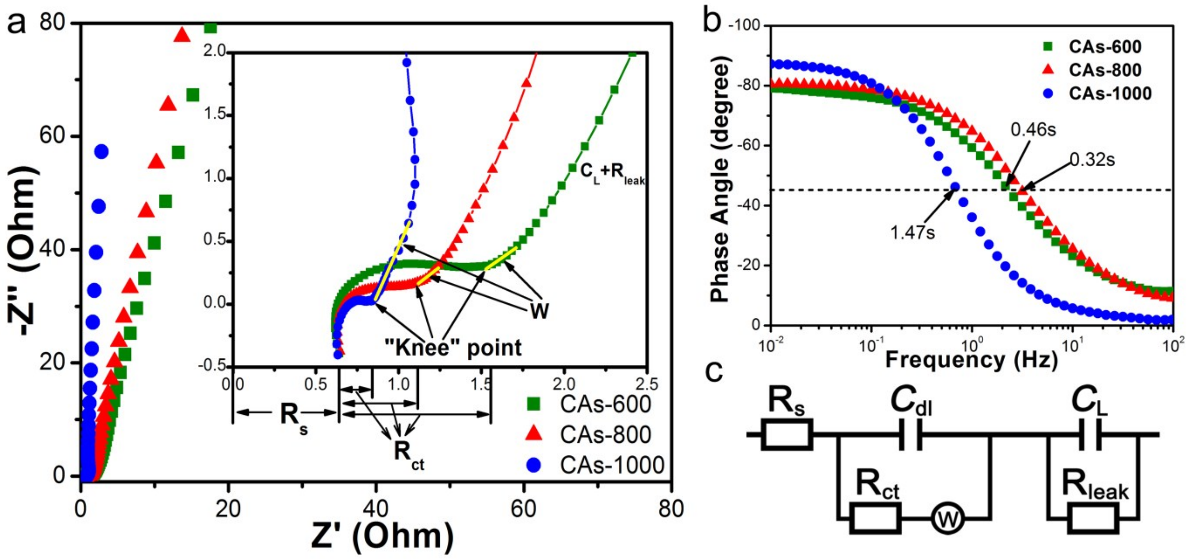

Figure S11. Electrochemical impedance spectroscopy data. (a) The Nyquist plots of CAs. The inset in (a) shows the magnified high-frequency region and the resistor and capacitor elements in an equivalent circuit related to the specific parts. (b) Bode plots of phase angle versus frequency CAs-600, CAs-800 and CAs-1000. (c) The Randles equivalent circuit. The equivalent circuit is used to fit the Nyquist spectra.

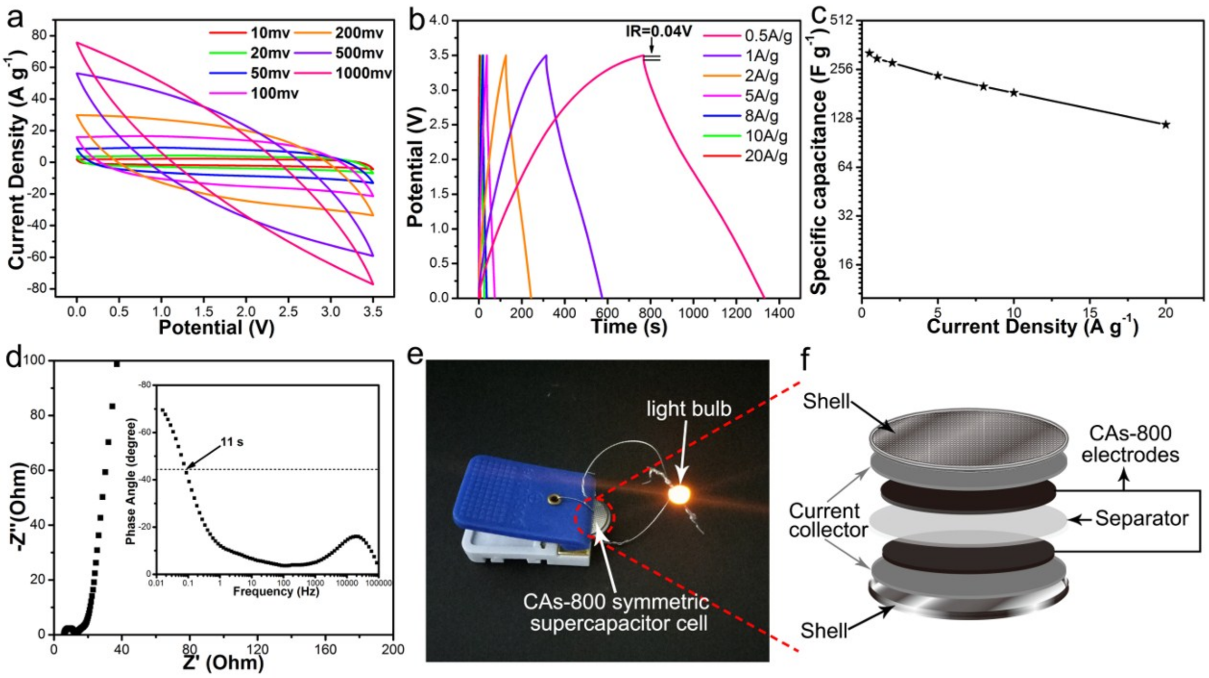

Figure S12. Bode plots of phase angle versus frequency CAs-600, CAs-800 and CAs1000. (f) Schematic illustration of the structure of the fabricated symmetric two-electrode supercapacitor cell.

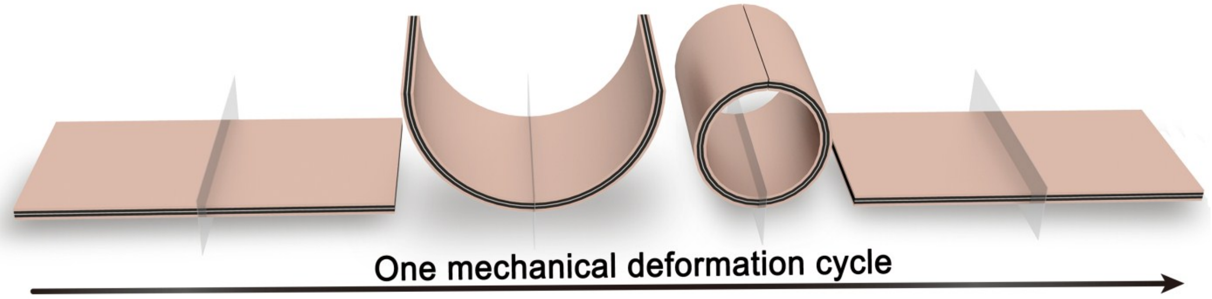

Figure S13. Bode plots of phase angle versus frequency CAs-600, CAs-800 and CAs-1000.

Supplementary Note 1

Figure S4 shows the FTIR spectrum of CAAs. The broad and strong band at 3420 cm $^{-1}$ was attributed to the O–H stretching vibrations, and the relatively weak bands at 2920 and 1400 cm $^{-1}$ were assigned to the stretching and deformation vibrations of aliphatic C–H. The two well absorption bands centered at 1700 and 1630 cm $^{-1}$ were ascribed to the C=O and C=C stretching vibrations, respectively, which corresponded to the carbonyl, quinone, ester or carboxyl,[1, 2] indicating that dehydration and aromatization processes taken place during the hydrothermal carbonization.

Supplementary Note 2

Electrochemical impedance spectroscopy (EIS) is a very useful method to analyze electrolyte ion transport and other electrochemical behavior. The Nyquist plots obtained from EIS analysis of the frequency range from 10^5 Hz to 10^{-2} Hz yields for three CAs electrodes were showed in the Figure S11a. The plots of these electrode materials feature a nearly vertical curve, indicating a typical capacitive behavior. The points at which the curve intersects the real axis (Z') in the Nyquist plot corresponds to the equivalent series resistances (ESR), which represent mainly intrinsic resistances (R_s) of the electrolyte and the electrical conductivity of the electrode. From the magnified data in the high-frequency range (Figure S11a, inset), these R_s are ≈ 0.68 Ω for them showing close to ideal conductivity in aqueous electrolytes (6 M KOH). The small near semicircles in all samples, reflecting the interfacial charge transfer resistance (R_{ct}) and double layer capacitance (C_{dl}), are observed that their diameters reduce as increasing carbonization temperature from 600 to 1000 °C. The CAs-1000 has a smallest semicircle complementally indicating its highest electron conductivity. After the semicircle, the transmission line with an angle of ≈45° to the x-axis from high frequency to the mid-frequency represents the Warburg region (W).[3] The more abundant porous CAs-800 exhibits the most efficient electrolyte ion diffusion in all electrodes, which contributes to easily access electrolyte ions without a diffusion limit. In contrast, the more intra-layer condensation of CAs-1000 leads to increase the resistance and restrained capacitances. In order to better understand the interfacial electrochemical behavior of the supercapacitors, we fit the Nyquist plots to an equivalent circuit (Figure S11c), where C_l is the low frequency mass capacitance and R_{leak} is the leakage resistance. The Bode plot provides useful insight into the rate capability of porous carbon materials. The characteristic frequency (f_0), whose reciprocal represents the time constant (τ_0), at the phase angle of −45° (Figure S11b) marks the transition point from resistive behavior to capacitive behavior. The τ_0 for the CAs-800 electrode is 0.32 s (f_0= 3.16 Hz), which is lowest than 0.46 s (f_0= 2.15 Hz) of CAs-600, and the longest time is 1.47 s (f_0= 0.68 Hz) of CAs-1000 likely resulting from the worst porosity. The results indicate high rate capability, low charge transfer resistance, and efficient electrolyte diffusion inside the CAs-800 electrodes.

Supplementary Note 3

In order to complement the evaluation of electrochemical performance of CAs-800, the symmetric two-electrode supercapacitor cell was assembled with 1-butyl-3-methyl-imidazolium tetrafluoroborate (BMIM BF_4) as the electrolyte, as shown schematically in Figure S12. CV curves taken at scan rates from 10 to 1000 mv s^{-1} are shown in Figure S12a, in which the curves are quasi-rectangular at the relatively low scan rate (<100 mv s^{-1}). The rectangular-like characteristics deforms slightly with the enhancement of scan rate, which may originate in insufficient time for ion diffusion and electron transfer in the ionic liquid electrolyte, suggesting the transition from capacitor behavior to resistor-like behavior need a relatively long time. As expected, the τ_0 obtained by EIS analysis is relatively long (= 11 s), as shown in the Figure S12d. The galvanostatic charge/discharge curves (Figure S12b) exhibit the quasi-symmetric capacitive behavior from 0 to 3.5 V at different current density. The specific capacitances calculated by the discharge branches are similar excellent compared with that of three-electrode test, as summarized in Figure S12c. The cell can be used to power for light-emitting diodes (LED), and lit beyond 5 minutes (Figure 6e). the assembled schematic is exhibited in Figure S12f.

Reference

1. M. Sevilla and A. B. Fuertes, *Carbon*, 2009, **47**, 2281–2289.
2. M. Sevilla and A. B. Fuertes, *Chem-Eur. J.*, 2009, **15**, 4195–4203.
3. Y. Shao, M. F. El-Kady, C. W. Lin, G. Zhu, K. L. Marsh, J. Y. Hwang, Q. Zhang, Y. Li, H. Wang and R. B. Kaner, *Adv. Mater.*, 2016, **28**, 6719–6726.